

Baryon Elastic and Transition Form Factors

Jorge Segovia

INP at Nanjing University, and
Pablo de Olavide University, Seville



Mass in the Standard Model and Consequences of its Emergence

ECT* Workshop April 19-23, 2021

Emergence

Low-level rules producing high-level phenomena with enormous apparent complexity

Start from the QCD Lagrangian:

$$\mathcal{L}_{\text{QCD}} = \bar{\psi}(i\not{D}-m)\psi - \frac{1}{4} G_a^{\mu\nu} G_{\mu\nu}^a + \frac{1}{2\xi} (\partial^\mu A_\mu^a)^2 + \partial^\mu \bar{c}^a \partial_\mu c^a + g f^{abc} (\partial^\mu \bar{c}^a) A_\mu^b c^c.$$



Lattice-regularized QCD, Continuum Schwinger-function methods, ...

And obtain:

- ☞ Dynamical generation of fundamental mass scale in pure Yang-Mills (gluon mass).
- ☞ Quark constituent masses and dynamical chiral symmetry breaking.
- ☞ Bound state formation: mesons, baryons, glueballs, hybrids, multiquark systems...
- ☞ Signals of confinement.

These (emergent) phenomena is not apparent in the QCD Lagrangian; however, they characterized the nonperturbative regime of QCD where hadrons live

Emergent phenomena could be associated with dramatic, dynamically driven changes in the analytic structure of QCD's Schwinger functions, which are solutions of the DSEs

Quark propagator:

$$\text{---}\bigcirc\text{---}^{-1} = \text{---}^{-1} + \text{---}\bigcirc\text{---}$$

Ghost propagator:

$$\text{---}\bigcirc\text{---}^{-1} = \text{---}^{-1} + \text{---}\bigcirc\text{---}$$

Ghost-gluon vertex:

$$\text{---}\bigcirc\text{---} = \text{---}\bigcirc\text{---} + \text{---}\bigcirc\text{---}$$

Gluon propagator:

$$\text{---}\bigcirc\text{---}^{-1} = \text{---}\bigcirc\text{---}^{-1} + \text{---}\bigcirc\text{---} + \text{---}\bigcirc\text{---} + \text{---}\bigcirc\text{---} + \text{---}\bigcirc\text{---} + \text{---}\bigcirc\text{---}$$

Quark-gluon vertex:

$$\text{---}\bigcirc\text{---} = \text{---}\bigcirc\text{---} + \text{---}\bigcirc\text{---} + \text{---}\bigcirc\text{---} + \text{---}\bigcirc\text{---} + \text{---}\bigcirc\text{---} + \text{---}\bigcirc\text{---} + \text{---}\bigcirc\text{---} + \text{---}\bigcirc\text{---}$$

Non-perturbative QCD: Dynamical generation of gluon mass

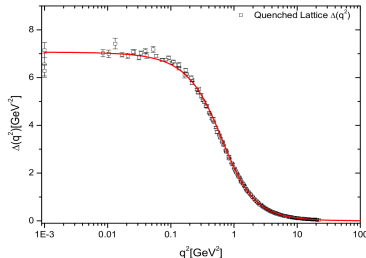
☞ Dressed-gluon propagator in Landau gauge:

$$i\Delta_{\mu\nu} = -iP_{\mu\nu}\Delta(q^2), \quad P_{\mu\nu} = g_{\mu\nu} - q_\mu q_\nu / q^2$$

- An inflexion point at $q^2 > 0$.
- Breaks the axiom of reflexion positivity.
- Gluon mass generation \leftrightarrow Schwinger mechanism.

A.C. Aguilar *et al.*, Phys. Rev. D78 (2008) 025010;

I.L. Bogolubsky *et al.*, Phys. Lett. B676 (2009) 69.



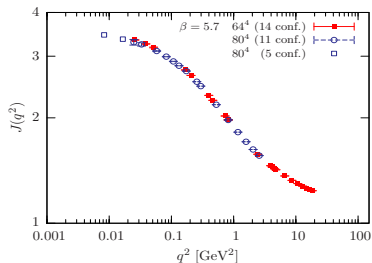
☞ Dressed-ghost propagator in Landau gauge:

$$G^{ab}(q^2) = \delta^{ab} \frac{J(q^2)}{q^2}$$

- No power-like singular behavior at $q^2 \rightarrow 0$.
- Good indication that $J(q^2)$ reaches a plateau.
- Saturation of ghost's dressing function.

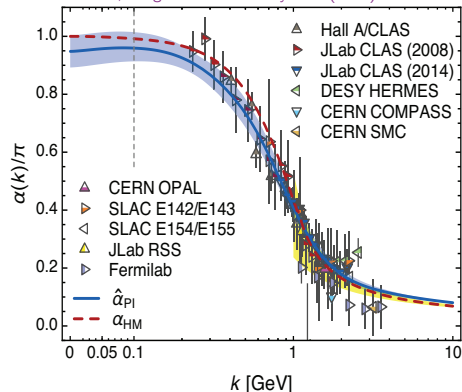
Ph. Boucaud *et al.*, JHEP 0806 (2008) 099;

C. Fischer *et al.*, Annals Phys. 324 (2009) 2408.



Non-perturbative QCD: Saturation at IR of process-independent effective-charge

D. Binosi *et al.*, Phys. Rev. D96 (2017) 054026;
A. Deur *et al.*, Prog. Part. Nucl. Phys. 90 (2016) 1-74.



⚡ Perturbative regime:

$$\alpha_{g_1}(k^2) = \alpha_{\overline{\text{MS}}}(k^2) \left[1 + 1.14 \alpha_{\overline{\text{MS}}}(k^2) + \dots \right]$$

$$\hat{\alpha}_{\text{PI}}(k^2) = \alpha_{\overline{\text{MS}}}(k^2) \left[1 + 1.09 \alpha_{\overline{\text{MS}}}(k^2) + \dots \right]$$

⚡ Data = running coupling defined from the Bjorken sum-rule.

$$\int_0^1 dx \left[g_1^p(x, k^2) - g_1^n(x, k^2) \right] = \frac{g_A}{6} \left[1 - \frac{1}{\pi} \alpha_{g_1}(k^2) \right]$$

⚡ Curve determined from combined continuum and lattice analysis of QCD's gauge sector (massless ghost and massive gluon).

⚡ The curve is a running coupling that does NOT depend on the choice of observable.

- No parameters.
- No matching condition.
- No extrapolation.

⚡ It predicts and unifies an enormous body of empirical data via the matter-sector bound-state equations.

Non-perturbative QCD: Dynamical generation of quark mass

☞ Dressed-quark propagator in Landau gauge:

$$S^{-1}(p) = Z_2(i\gamma \cdot p + m) + \Sigma(p) = \left(\frac{Z(p^2)}{i\gamma \cdot p + M(p^2)} \right)^{-1}$$

- Mass generated from the interaction of quarks with the gluon-medium.
- Light quarks acquire a **HUGE** constituent mass.
- Responsible of the 98% of proton's mass, the large splitting between parity partners, ...

☞ Goldberger-Treiman relation at the quark level:

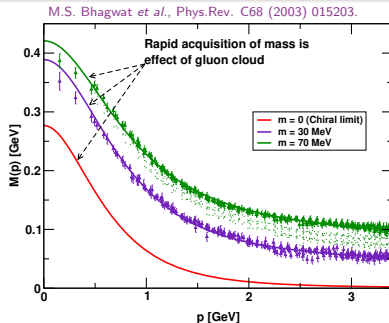
Quark propagator: $S^{-1}(p) = i\gamma \cdot p A(p^2) + B(p^2),$

Pion's BS-amplitude: $\Gamma_\pi(p, P) \propto \gamma^5 E_\pi(p; P).$

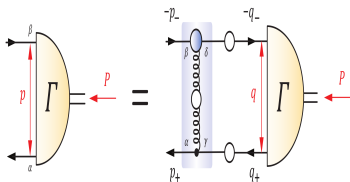
$$f_\pi E_\pi(p; 0) = B(p^2)$$

Properties of the massless pion are a direct measure of the dressed-quark mass function

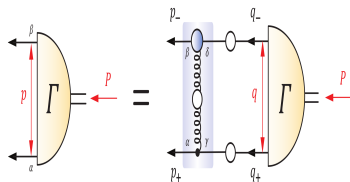
Cleanest expression of the mechanism that is responsible for almost all the visible mass in the universe



Any interaction able to create Goldstone modes as bound-states of light dressed-quark and -antiquark will generate strong $\bar{3}_c$ correlations between any two dressed quarks.



Meson BSE



Diquark BSE

☞ Owing to properties of charge-conjugation, a diquark with spin-parity J^P may be viewed as a partner to the analogous J^{-P} meson:

$$\Gamma_{q\bar{q}}(p; P) = - \int \frac{d^4 q}{(2\pi)^4} g^2 D_{\mu\nu}(p - q) \frac{\lambda^a}{2} \gamma_\mu S(q + P) \Gamma_{q\bar{q}}(q; P) S(q) \frac{\lambda^a}{2} \gamma_\nu$$

$$\Gamma_{qq}(p; P) C^\dagger = - \frac{1}{2} \int \frac{d^4 q}{(2\pi)^4} g^2 D_{\mu\nu}(p - q) \frac{\lambda^a}{2} \gamma_\mu S(q + P) \Gamma_{qq}(q; P) C^\dagger S(q) \frac{\lambda^a}{2} \gamma_\nu$$

☞ Whilst no pole-mass exists, the following mass-scales express the strength and range of the correlation:

$$m_{[ud]_{0+}} = 0.7 - 0.8 \text{ GeV}, \quad m_{\{uu\}_{1+}} = 0.9 - 1.1 \text{ GeV}, \quad m_{\{dd\}_{1+}} = m_{\{ud\}_{1+}} = m_{\{uu\}_{1+}}$$

☞ Diquark correlations are soft, they possess an electromagnetic size:

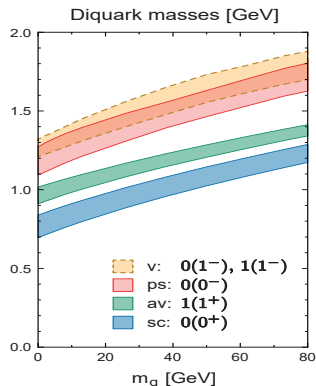
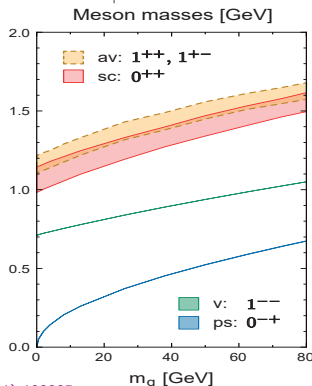
$$r_{[ud]_{0+}} \gtrsim r_\pi, \quad r_{\{uu\}_{1+}} \gtrsim r_\rho, \quad r_{\{uu\}_{1+}} > r_{[ud]_{0+}}$$

Octet and decuplet baryons

	[nn]	{nn}	[ns]	{ns}	{ss}
N	●	●			
Δ		●			
Λ	●		●	●	
Σ		●	●	●	
Ξ			●	●	●
Ω					●

Other baryons as parity partners

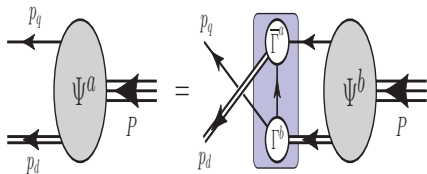
- ☞ $[I = 0, J^P = 0^+]$: Isoscalar-scalar.
- ☞ $[I = 1, J^P = 1^+]$: Isovector-pseudovector.
- ☞ $[I = 0, J^P = 0^-]$: Isoscalar-pseudoscalar.
- ☞ $[I = 0, J^P = 1^-]$: Isoscalar-vector.
- ☞ $[I = 1, J^P = 1^-]$: Isovector-vector.



The quark+diquark structure of a baryon

A baryon can be viewed as a **Borromean bound-state**, the binding within which has two contributions:

- Formation of tight diquark correlations.
- Quark exchange depicted in the shaded area.



The exchange ensures that diquark correlations within the baryon are **fully dynamical**: no quark holds a special place.

The rearrangement of the quarks guarantees that the baryon's wave function complies with **Pauli statistics**.

The number of states in the **spectrum of baryons obtained is similar** to that found in the three-constituent quark model, just as it is in today's LQCD calculations.

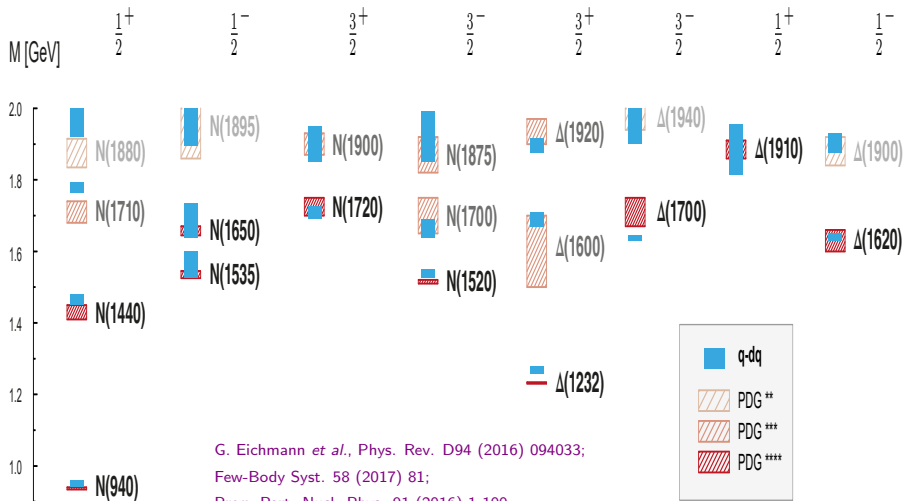
Modern diquarks are **different from the old static, point-like diquarks** which featured in early attempts to explain the so-called missing resonance problem.

Modern diquarks enforce certain **distinct interaction patterns** for the singly- and doubly-represented valence-quarks within the baryon.

S.-S. Xu *et al.*, Phys. Rev. D92 (2015) 114034; Y. Lu *et al.*, Phys. Rev. C96 (2017) 015208;
C. Chen *et al.*, Phys. Rev. D100 (2019) 054009; P.-L. Yin *et al.*, Phys. Rev. D100 (2019) 034008.

Baryon spectrum within the quark+diquark picture

- ☞ Spectrum in one to one agreement with experiment.
- ☞ Correct level ordering (without coupled-channels effects).



non-relativistic

Mesons: $P = (-1)^{L+1}$

S	L	J^{PC}
0	0	0^{-+}
1	0	1^{--}
0	1	1^{+-}
1	1	0^{++}



relativistic

~~$$P = (-1)^{L+1}$$~~

Bethe, Salpeter, Llewellyn-Smith 1950ies

$$\Gamma_\pi(P, p) = \gamma_5 [F_1(P, p) \quad \text{s-wave} \\ + F_2(P, p) i \not{p} \\ + F_3(P, p) p \not{P} i \not{p} \quad \text{p-wave} \\ + F_4(P, p) [\not{p}, \not{P}]]$$

Baryons: $P = (-1)^L$

S	L	J^P
1/2	0	$1/2^+$
3/2	2	

~~$$P = (-1)^L$$~~

J^P	total				
		s-wave	p-wave	d-wave	f-wave
$1/2^+$	64	8	36	20	
$3/2^+$	128	4	36	60	28

Transition form factors of nucleon resonances

Unique window into their
quark and gluon structure

Distinctive information on the
roles played by emergent
phenomena in QCD

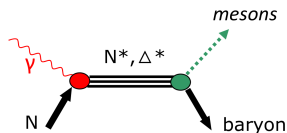
Broad range of
photon virtuality

Probe the excited nucleon
structures at perturbative and
non-perturbative QCD scales

A vigorous experimental program has been and is still under way worldwide
CLAS, CBELSA, GRAAL, MAMI and LEPS

- ☞ Multi-GeV polarized cw beam, large acceptance detectors, polarized proton/neutron targets.
- ☞ Very precise data for 2-body processes in wide kinematics (angle, energy): $\gamma p \rightarrow \pi N$, ηN , $K Y$.
- ☞ More complex reactions needed to access high mass states: $\pi\pi N$, $\pi\eta N$, ωN , ϕN , ...

Extract s-channel resonances



Nucleon Resonance Photo-/Electrocouplings Determined from Analyses of Experimental Data on Exclusive Meson Electroproduction off Protons

Definition (docx) of $A_{1/2}$, $A_{3/2}$ and $S_{1/2}$ electrocouplings
(in pdf format)

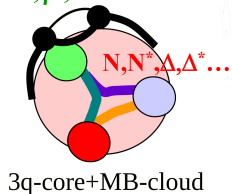
Links to the files with electrocoupling values (docx marked by resonance symbols/unmarked pdf)

Δ(1232)3/2⁺	N(1440)1/2⁺	N(1520)3/2⁻	N(1535)1/2⁻	Δ(1620)1/2⁻	N(1650)1/2⁻
pdf	pdf	pdf	pdf	pdf	pdf
N(1675)5/2⁻	N(1680)5/2⁺	Δ(1700)3/2⁻	N(1710)1/2⁺	N(1720)3/2⁺	
pdf	pdf	pdf	pdf	pdf	

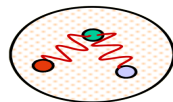
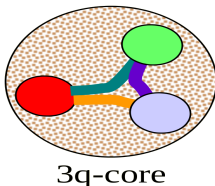
https://userweb.jlab.org/~mokeev/resonance_electrocouplings/

CLAS12 aims to measure the N^* photo- and electro-couplings at Q^2 ever achieved so far and thus trying to distinguish between different effective degrees of freedom.

$\pi, \rho, \omega \dots$

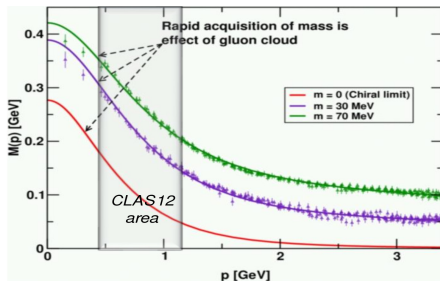


Low Q^2



High Q^2

CLAS12 will be able to extract information about fundamental quantities in QCD at an intermediate energy region.



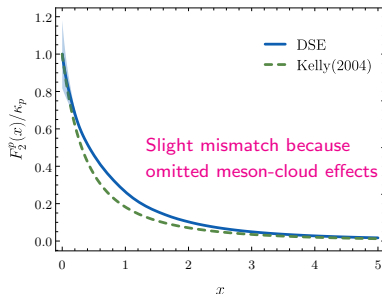
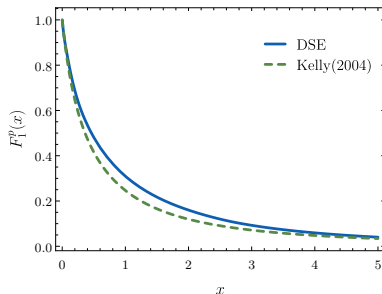
$$\gamma^* N(940)\frac{1}{2}^+ \rightarrow N(940)\frac{1}{2}^+$$

Based on:

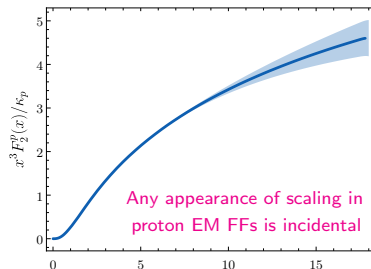
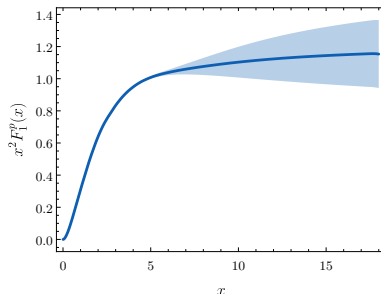
- **Nucleon elastic form factors at accessible large spacelike momenta**
Z.-F. Cui, C. Chen, D. Binosi, F. De Soto, C.D. Roberts, J. Rodríguez-Quintero, S.M. Schmidt and J. Segovia
Phys. Rev. D102 (2020) 014043, arXiv:hep-ph/2003.11655
- **PDAs: Revealing correlations within the proton and Roper**
C. Mezrag, J. Segovia, L. Chang and C.D. Roberts
Phys. Lett. B783 (2018) 263-267, arXiv:nucl-th/1711.09101
- **Understanding the nucleon as a borromean bound-state**
J. Segovia, C.D. Roberts and S.M. Schmidt
Phys. Lett. B750 (2015) 100-106, arXiv:nucl-th/1506.05112
- **Nucleon and Delta elastic and transition form factors**
J. Segovia, I.C. Cloët, C.D. Roberts and S.M. Schmidt
Few-Body Syst. 55 (2014) 1185-1222, arXiv:nucl-th/1408.2919

Proton's Dirac and Pauli form factors

Comparison with experiment:

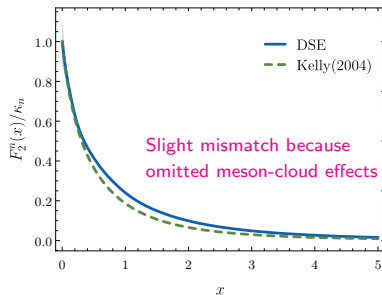
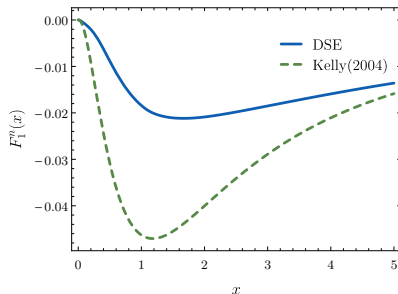


Comparison with perturbative QCD:

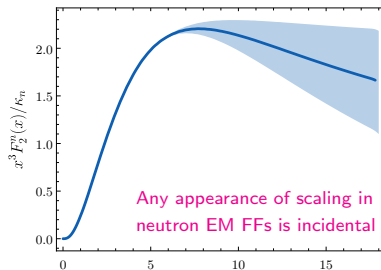
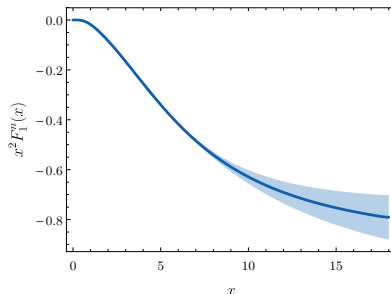


Neutron's Dirac and Pauli form factors

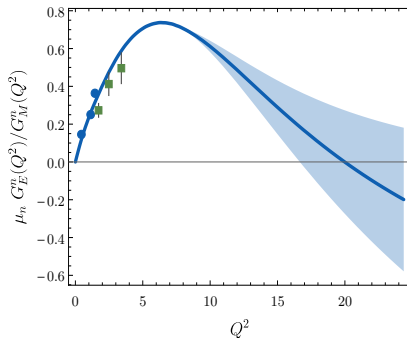
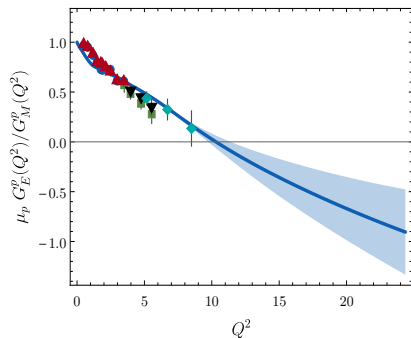
Comparison with experiment:



Comparison with perturbative QCD:



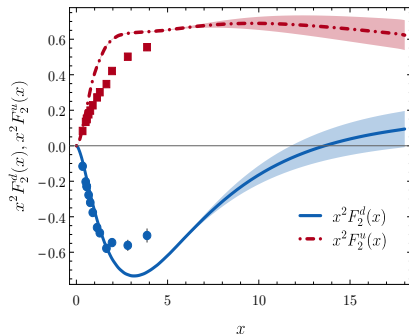
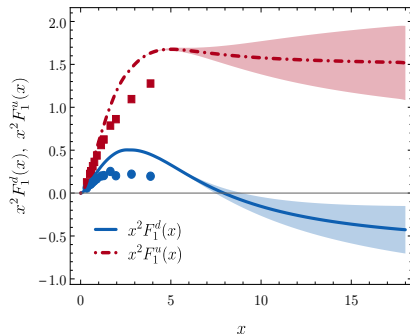
Unit-normalized ratio of Sachs electric and magnetic form factors



Observations:

- There is no evidence for scaling in Dirac and Pauli form factors, and thus in the electromagnetic Sachs form factors.
- Our analysis predicts a zero for the proton's electromagnetic ratio at $Q^2 = 10.3^{+1.1}_{-0.7} \text{ GeV}^2$.
- The neutron's electromagnetic ratio has a peak at $Q^2 \approx 6 \text{ GeV}^2$ and then crossed zero for $Q^2 = 20.1^{+10.6}_{-3.5} \text{ GeV}^2$.
- All these features can be related with both quark-quark and angular momentum correlations within the nucleon.

Z.-F. Cui *et al.*, Phys. Rev. D102 (2020) 014043.



Observations:

- F_1^d is smaller than F_1^u , even allowing for the difference in normalisation, and decreases more quickly as x increases.
- The location of the zero in F_1^d is a measure of the relative probability of finding pseudovector and scalar diquarks in the proton.
- The u - and d -quark Pauli form factors are roughly equal in magnitude on $x \lesssim 5$; i.e. F_2^d is suppressed with respect F_2^u but only at large momentum transfer.
- There are contributions playing an important role in F_2 , like the anomalous magnetic moment of dressed-quarks or meson-baryon final-state interactions.

$$\gamma^* N(940) \frac{1}{2}^+ \rightarrow N(1440) \frac{1}{2}^+$$

Based on:

- **Nucleon-to-Roper electromagnetic transition form factors at large Q^2**
C. Chen, Y. Lu, D. Binosi, C.D. Roberts, J. Rodríguez-Quintero, and J. Segovia
Phys. Rev. D99 (2019) 034013, arXiv:nucl-th/1811.08440
- **Structure of the nucleon's low-lying excitations**
C. Chen, B. El-Bennich, C.D. Roberts, S.M. Schmidt, J. Segovia and S. Wan
Phys. Rev. D97 (2018) 034016, arXiv:nucl-th/1711.03142
- **Dissecting nucleon transition electromagnetic form factors**
J. Segovia and C.D. Roberts
Phys. Rev. C94 (2016) 042201(R), arXiv:nucl-th/1607.04405
- **Completing the picture of the Roper resonance**
J. Segovia, B. El-Bennich, E. Rojas, I.C. Cloët, C.D. Roberts, S.-S. Xu and H.-S. Zong
Phys. Rev. Lett. 115 (2015) 171801, arXiv:nucl-th/1504.04386

Nucleon's first radial excitation in DSEs

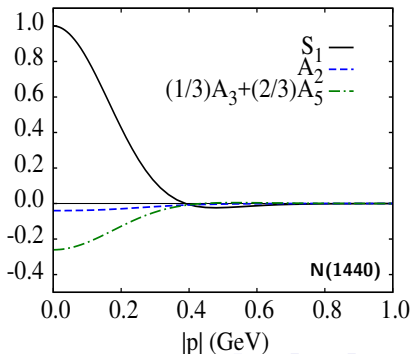
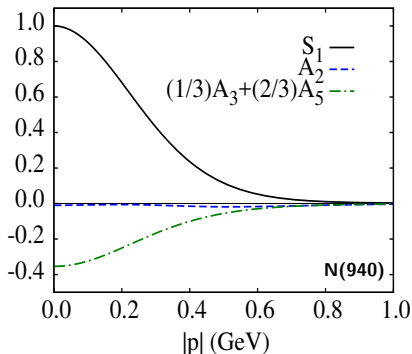
Bare-states of nucleon resonances correspond to hadron structure calculations which exclude the coupling with the meson-baryon final-state interactions

$$M_{Roper}^{DSE} = 1.73 \text{ GeV} \quad M_{Roper}^{EBAC} = 1.76 \text{ GeV}$$

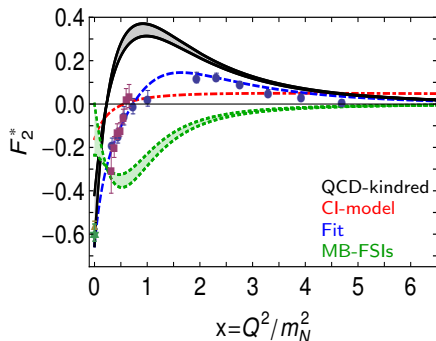
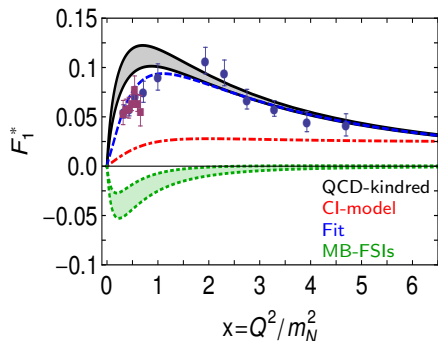
Observations:

- Meson-Baryon final state interactions reduce dressed-quark core mass by 20%.
- Roper and Nucleon have very similar wave functions and diquark content.
- A single zero in S-wave components of the wave function \Rightarrow A radial excitation.

0th Chebyshev moment of the S-wave components



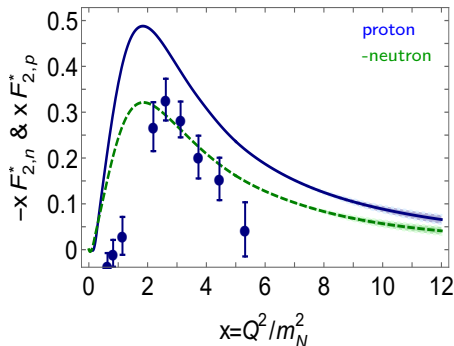
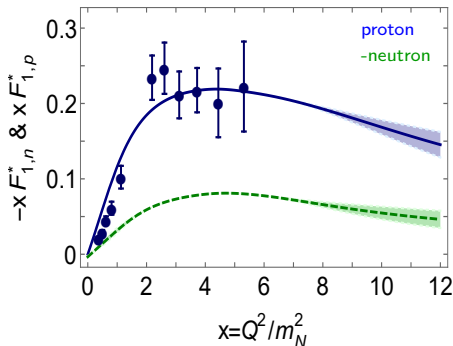
Nucleon-to-Roper transition form factors at high virtual photon momenta penetrate the meson-cloud and thereby illuminate the dressed-quark core



Observations:

- Our calculation agrees quantitatively in magnitude and qualitatively in trend with the data on $x \gtrsim 2$.
- The mismatch between our prediction and the data on $x \lesssim 2$ is due to meson cloud contribution.
- The dotted-green curve is an inferred form of meson cloud contribution from the fit to the data.

CLAS12 detector at JLab will deliver data on the Roper-resonance electroproduction form factors out to $Q^2 \sim 12m_N^2$ in both the charged and neutral channels



Observations:

- On the domain depicted, there is no indication of the scaling behavior expected of the transition form factors: $F_1^* \sim 1/x^2$, $F_2^* \sim 1/x^3$.
- Since each dressed-quark in the baryons must roughly share the momentum, Q , we expect that such behaviour will only become evident on $x \gtrsim 20$.

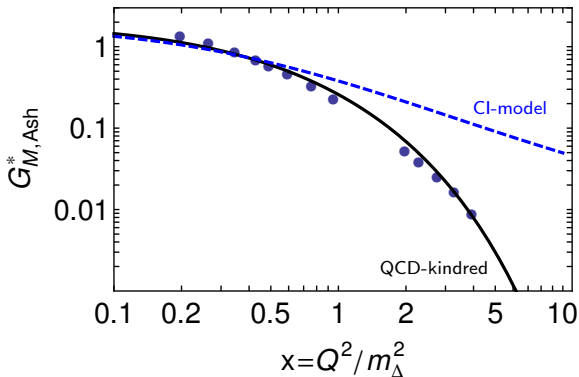
$$\gamma^* N(940)_{\frac{1}{2}}^{+} \rightarrow \Delta(1232)_{\frac{3}{2}}^{+}$$

Based on:

- **Dissecting nucleon transition electromagnetic form factors**
J. Segovia and C.D. Roberts
Phys. Rev. C94 (2016) 042201(R), arXiv:nucl-th/1607.04405
- **Nucleon and Delta elastic and transition form factors**
J. Segovia, I.C. Cloët, C.D. Roberts and S.M. Schmidt
Few-Body Syst. 55 (2014) 1185-1222, arXiv:nucl-th/1408.2919
- **Elastic and transition form factors of the $\Delta(1232)$**
J. Segovia, C. Chen, I.C. Cloët, C.D. Roberts, S.M. Schmidt and S. Wan
Few-Body Syst. 55 (2014) 1-33, arXiv:nucl-th/1308.5225
- **Insights into the $\gamma^* N \rightarrow \Delta$ transition**
J. Segovia, C. Chen, C.D. Roberts and S. Wan
Phys. Rev. C88 (2013) 032201(R), arXiv:nucl-th/1305.0292

Presentations of experimental data typically use the Ash convention

– $G_{M,Ash}^(Q^2)$ falls faster than a dipole –*



☞ No sound reason to expect:

$$G_{M,Ash}^*/G_M \sim \text{constant}$$

☞ Jones-Scadron must exhibit:

$$G_{M,J-S}^*/G_M \sim \text{constant}$$

☞ Meson-cloud effects

- Up-to 35% for $Q^2 \lesssim 2.0m_{\Delta}^2$.
- Soft \rightarrow disappear rapidly.

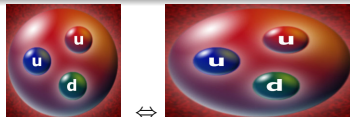
☞ $G_{M,Ash}^*$ vs $G_{M,J-S}^*$

- A Difference of $1/\sqrt{Q^2}$.

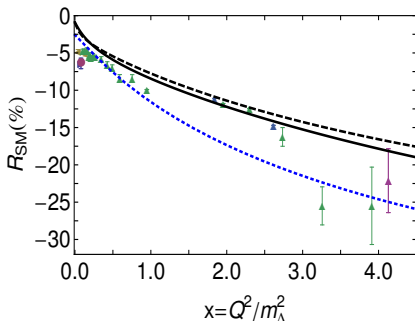
The electric- and coulomb-quadrupole ratios

☞ $R_{EM} = R_{SM} = 0$ in SU(6)-symmetric CQM.

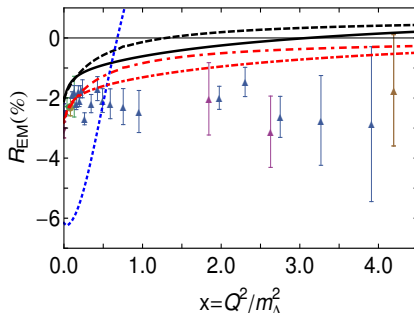
- Deformation of the hadrons involved.
- Modification of the transition current.



☞ R_{SM} : Good description of the rapid fall at large momentum transfer.



☞ R_{EM} : A particularly sensitive measure of orbital angular momentum correlations.



☞ *Zero Crossing in the electric transition form factor:*

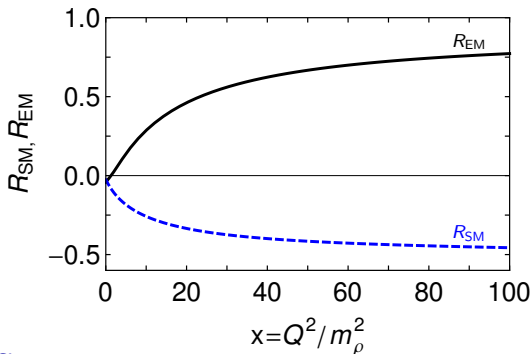
Contact interaction $\rightarrow Q^2 \sim 0.75m_\Delta^2 \sim 1.14 \text{ GeV}^2$

QCD-kindred interaction $\rightarrow Q^2 \sim 3.25m_\Delta^2 \sim 4.93 \text{ GeV}^2$

Helicity conservation arguments in pQCD should apply equally to:

- *Results obtained within our QCD-kindred framework;*
- *Results produced by a symmetry-preserving treatment of a contact interaction.*

$$R_{EM} \stackrel{Q^2 \rightarrow \infty}{\Rightarrow} 1, \quad R_{SM} \stackrel{Q^2 \rightarrow \infty}{\Rightarrow} \text{constant}.$$



Observations:

- Truly asymptotic Q^2 is required before predictions are realized.
- $R_{EM} = 0$ at an empirical accessible momentum and then $R_{EM} \rightarrow 1$.
- $R_{SM} \rightarrow \text{constant}$. Curve contains the logarithmic corrections expected in QCD.

$$\gamma^* N(940) \frac{1}{2}^+ \rightarrow \Delta(1600) \frac{3}{2}^+$$

Based on:

- **Transition form factors: $\gamma + p \rightarrow \Delta(1232), \Delta(1600)$**
Y. Lu, C. Chen, Z.-F. Cui, C.D. Roberts, S.M. Schmidt, J. Segovia, H.-S. Zong
Phys. Rev. D100 (2019) 034001, arXiv:nucl-th/1904.03205
- **Masses of ground-state mesons and baryons, including those with heavy quarks**
P.-L. Yin, C. Chen, G. Krein, C.D. Roberts, J. Segovia and S.-S. Xu
Phys. Rev. D100 (2019) 054009, arXiv:nucl-th/1901.04305
- **Spec. and struc. of octet and decuplet and their positive-parity excitations**
C. Chen, G. Krein, C.D. Roberts, S.M. Schmidt and J. Segovia
Phys. Rev. D100 (2019) 054009, arXiv:nucl-th/1901.04305
- **Parity partners in the baryon resonance spectrum**
Y. Lu, C. Chen, C.D. Roberts, J. Segovia, S.-S. Xu and H.-S. Zong
Phys. Rev. C96 (2017) 015208, arXiv:nucl-th/1705.03988

Wave function decomposition: $N(1440)$ cf. $\Delta(1600)$

	$N(940)$	$N(1440)$	$\Delta(1232)$	$\Delta(1600)$
scalar	62%	62%	—	—
pseudovector	29%	29%	100%	100%
mixed	9%	9%	—	—
S -wave	0.76	0.85	0.61	0.30
P -wave	0.23	0.14	0.22	0.15
D -wave	0.01	0.01	0.17	0.52
F -wave	—	—	~ 0	0.02

$N(1440)$

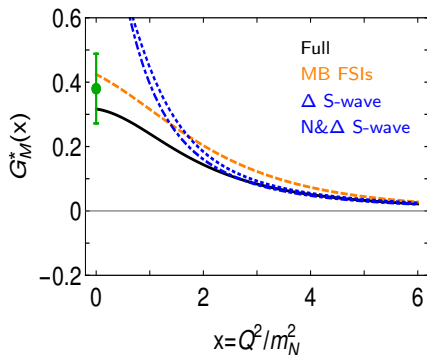
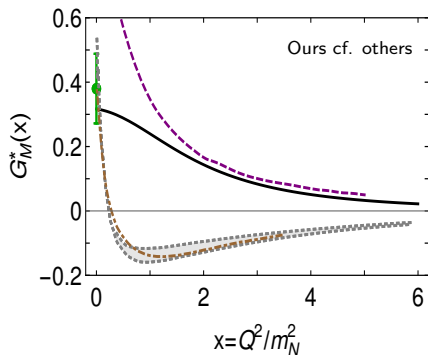
- Roper's diquark content are almost identical to the nucleon's one.
- It has an orbital angular momentum composition which is very similar to the one observed in the nucleon.

$\Delta(1600)$

- $\Delta(1600)$'s diquark content are almost identical to the $\Delta(1232)$'s one.
- It shows a dominant $\ell = 2$ angular momentum component with its S -wave term being a factor 2 smaller.

The presence of all angular momentum components compatible with the baryon's total spin and parity is an inescapable consequence of solving a realistic Poincaré-covariant Faddeev equation

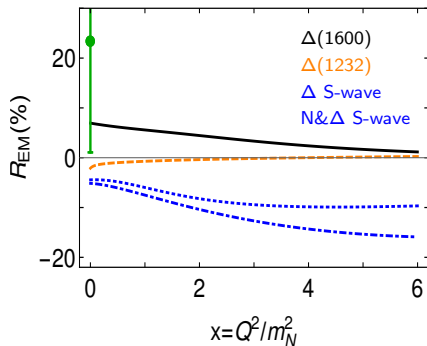
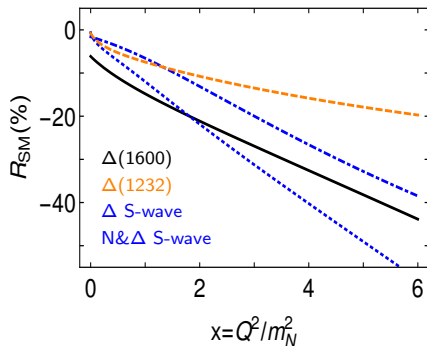
The magnetic dipole form factor in the Jones-Scadron convention



Observations:

- It is positive defined in the whole range of photon momentum and decreases smoothly with larger Q^2 -values.
- The mismatch with the empirical result are comparable with that in the $\Delta(1232)$ case, suggesting that MB FSIs are of similar importance in both channels.
- Higher partial-waves have a visible impact on G_M^* : They bring the magnetic dipole moment to lower values which could be compatible with experiment.

The electric- and coulomb-quadrupole ratios



Observations:

- $R_{SM}' \gtrsim R_{SM}^{\Delta}$ indicating that higher orbital angular momentum components in the $\Delta(1600)$ are more important than in the $\Delta(1232)$.
- R_{EM} for the $\Delta(1600)$ transition is far larger in magnitude than the analogous result for the $\Delta(1232)$ (and opposite in sign).
- Points above are an observable manifestation of important higher orbital angular momentum components in both states.
- In particular, there is an enhanced D -wave strength in the $\Delta(1600)$ relative to that in the $\Delta(1232)$.

We insist on our purpose of getting an unified study of EM elastic and transition form factors of nucleon resonances using QCD-kindred kernels and interaction vertices

☞ The $\gamma^* N \rightarrow \text{Nucleon} [\equiv N(940)]$ reaction:

- Proton's and neutron's electromagnetic ratios are sensible observables to disentangle fundamental quantities of QCD.
- The presence of strong diquark correlations within the nucleon is sufficient to understand empirical extractions of the flavor-separated form factors.
- Scalar diquark dominance and the presence of higher orbital angular momentum components are responsible of the Q^2 -behaviour of G_E^p/G_M^p and F_2^p/F_1^p .

☞ The $\gamma^* N \rightarrow \text{Nucleon}' [\equiv N(1440)]$ reaction:

- The Roper is the proton's first radial excitation. It consists on a dressed-quark core augmented by a meson cloud that reduces its mass by approximately 20%.
- Our calculation agrees quantitatively in magnitude and qualitatively in trend with the data on $x \gtrsim 2$. The mismatch on $x \lesssim 2$ is due to meson-cloud contribution.
- CLAS12@JLab will test our predictions for the charged and neutral channels in a range of momentum transfer larger than 4.5 GeV^2 .

☞ The $\gamma^* N \rightarrow \text{Delta} [\equiv \Delta(1232)]$ reaction:

- $G_{M,J-S}^{*P}$ falls asymptotically at the same rate as G_M^P . This is compatible with isospin symmetry and pQCD predictions.
- Data do not fall unexpectedly rapid once the kinematic relation between Jones-Scadron and Ash conventions is properly account for.
- Limits of pQCD, $R_{EM} \rightarrow 1$ and $R_{SM} \rightarrow \text{constant}$, are apparent in our calculation but truly asymptotic Q^2 is required before the predictions are realized.

☞ The $\gamma^* N \rightarrow \text{Delta}' [\equiv \Delta(1600)]$ reaction:

- G_M^* and R_{EM} are consistent with the empirical values at the real photon point, but we expect inclusion of MB FSI to improve the agreement on $Q^2 \sim 0$
- R_{EM} is markedly different for $\Delta(1600)$ than for $\Delta(1232)$, highlighting the sensitivity of G_E^* to the degree of deformation of the Δ -baryons.
- R_{SM} is qualitatively similar for both $\gamma^* N \rightarrow \Delta(1600)$ and $\gamma^* N \rightarrow \Delta(1232)$ transitions, still larger (in absolute value) for the $\Delta(1600)$ case.